IOPscience iopscience.iop.org

Home Search Collections Journals About Contact us My IOPscience

The effects of inelastic scattering in open quantum dots: reduction of conductance fluctuations and disruption of wave-function `scarring'

This article has been downloaded from IOPscience. Please scroll down to see the full text article.

1996 J. Phys.: Condens. Matter 8 L667

(http://iopscience.iop.org/0953-8984/8/45/002)

View the table of contents for this issue, or go to the journal homepage for more

Download details:
IP Address: 171.66.16.207
The article was downloaded on 14/05/2010 at 04:27

Please note that terms and conditions apply.

J. Phys.: Condens. Matter **8** (1996) L667–L674. Printed in the UK

LETTER TO THE EDITOR

The effects of inelastic scattering in open quantum dots: reduction of conductance fluctuations and disruption of wave-function 'scarring'

R Akis†, J P Bird‡ and D K Ferry†

† Center for Solid State Electronics Research, Center for Systems Science and Engineering, and Department of Electrical Engineering, Arizona State University, Tempe, AZ 85287, USA

‡ Nanoelectronics Materials Laboratory, Frontier Research Program, RIKEN, 2-1 Hirosawa, Wako, Saitama 351-01, Japan

Received 15 August 1996

Abstract. We perform numerical simulations of the quantum mechanical transport and corresponding wave-functions in open, square quantum dots. The effects of inelastic scattering are introduced phenomenologically. Examining the root mean square amplitude of the conductance fluctuations, we find they decay exponentially with $1/\tau_\phi$ (τ_ϕ being the inelastic scattering time), in good agreement with the results of recent experiments. In previous work, we have found the wave-functions of such dots should be 'scarred'. We examine the robustness of this scarring effect to the phase-breaking process.

The electrical properties of mesoscopic devices are well known to be influenced by electron interference [1]. In disordered systems, electronic motion is diffusive and a significant understanding of the processes affecting the interference has already been achieved. Recent advances in semiconducting micro-processing technology now enable the fabrication of sub-micrometre scale quantum dots, in which electronic motion is predominantly ballistic [2–6]. While precise details differ between experiments, the devices usually consist of some central scattering region, patterned on a length scale smaller than the elastic mean free path, and connected to source and drain reservoirs via tunable quantum point contact leads. Large-angle scattering of electrons is restricted to the boundaries of these devices, and relatively little is known about the details of electron interference within them. Recent experiments suggest, however, that their electrical properties are dominated by a characteristic *periodicity* in their magnetoconductance, which is replicated as strong periodic oscillations in the fluctuation correlation function [6]. This periodicity arises from the remnants of regular, semi-classical orbits within the dot. Theoretical simulation of the quantum transport in these ballistic structures suggests that strong 'scarring' of the total wave-function is present in the dot. The scarring can correspond to the remnants of just a *single* classical orbit, which in turn gives rise to the *periodic* fluctuations in the low-field magneto-resistance of the devices [8].

In this letter, a stable iterative matrix approach [7] is employed to investigate the effect of finite phase breaking on the conductance fluctuations and on the wave-function scarring in these ballistic quantum dots [8]. The method we employ allows evaluation of both the dot conductance and the total wave-function. The phase breaking is accounted for in a phenomenological fashion, being quantified in terms of a corresponding inelastic

 © 1996 IOP Publishing Ltd

scattering time τ_ϕ. For infinite τ_ϕ at suitably low temperatures, the wave-function is found to be strongly scarred by the remnant of a single classical orbit, consistent with the periodic fluctuations observed in experiment [4]. With increasing phase breaking, however, the scarring is very rapidly destroyed. Simultaneously, the amplitude of the calculated conductance fluctuations decays exponentially as a function of $1/\tau_\phi$, in good agreement with the results of experiments. Such agreement provides clear evidence that the transport properties of mesoscopic devices can be strongly influenced by the quantum remnants of a small group of classical orbits. We therefore briefly consider the process by which these orbits come to dominate the transport characteristics.

For our simulations, the general situation is one in which ideal quantum wires, which extend outward to $\pm\infty$, are connected to a square quantum dot, with entry and exit ports aligned at the top. A magnetic field is applied normal to the plane of the dot. We solve this quantum mechanical problem on a discrete lattice using an iterative matrix method that is numerically stabilized variant of the transfer matrix approach. The discretized Schrödinger equation, keeping terms up to first order in the approximation of the derivative, has the form

$$\left(E_F - \mathbf{H}_j\right)\psi_j + \mathbf{H}_{j,j-1}\psi_{j-1} + \mathbf{H}_{j,j+1}\psi_{j+1} = 0 \tag{1}$$

where ψ_j is an M-dimensional vector containing the amplitudes of the jth slice. This problem is solved on a square lattice of lattice constant a with the wires extending M lattice sites across in the x direction. That is, the region of interest is broken down into a series of slices along the y direction. In this equation, the $\mathbf{H}_j$ matrices represent Hamiltonians for individual slices and the matrices $\mathbf{H}_{j,j-1}$ and $\mathbf{H}_{j,j+1}$ give the inter-slice coupling. By approximating the derivative, the kinetic energy terms of Schrödinger's equation are mapped onto a tight-binding model with $t = -\hbar^2/2m^*a^2$ representing nearest-neighbour hopping. The potential V at site i, j simply adds to the on-site energies, which appear along the diagonal of the $\mathbf{H}_j$ matrices. Transfer matrices based on (1) can then be derived, which allow translation across the system to obtain the transmission coefficients, and which, in turn, enter the Landauer–Büttiker formula to give the conductance. The instability problems inherent in the transfer matrix approach due to exponentially growing and decaying contributions of evanescent modes are overcome by some clever matrix manipulations [7]. Rather than just multiplying transfer matrices together, the scheme is turned into an iterative procedure that does not allow the eigenvalues to diverge.

The modification of this technique to take into account inelastic scattering and phase randomization can be performed phenomenologically by introducing an imaginary potential [9]. For an inelastic scattering time τ_ϕ the original potential V is modified to become $V - \mathrm{i}V_{in}$, where $V_{in} = \hbar/(2\tau_\phi)$. In our calculations, we impose the phase breaking only in the dot itself and not in the leads. One calculates the transmission and reflection coefficients as before. Current conservation is maintained in the presence of the imaginary potential since one can show that the current that is apparently lost from the propagating modes actually goes into an inelastic scattering channel. The total inelastic scattering current is given by

$$j_{in} = \left(1/\tau_\phi\right)\int\int \psi^*\psi\,\mathrm{d}s. \tag{2}$$

We assume that this inelastic channel current is equally divided between the two leads and add this to the results of the Landauer–Büttiker formula (which constitute the elastic contribution) to obtain the *total* conductance. The quantity of main interest to us here, the root mean square amplitude of the conductance fluctuations δg, can be obtained from the

correlation function,

$$F(\Delta B) = \langle [g(B) - \langle g(B)\rangle][g(B + \Delta B) - \langle g(B)\rangle]\rangle \tag{3}$$

where $g(B)$ is the conductance in units of e^2/h, B is the magnetic field, and the angle brackets indicate an average over a suitably large magnetic field range. The fluctuation amplitude is then given by $\delta g = [F(0)]^{1/2}$.

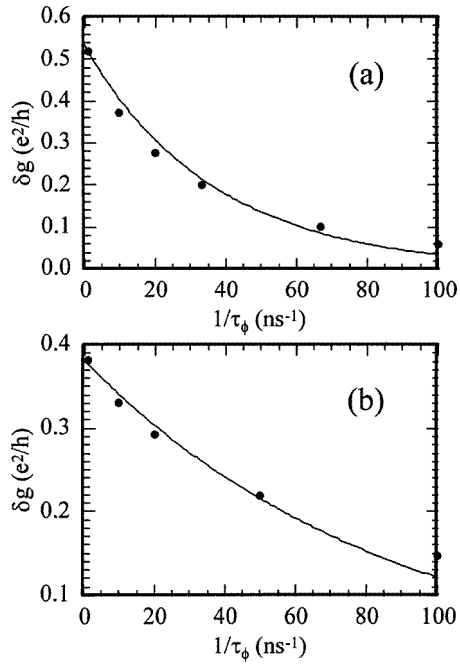

Figure 1. The root mean square average of the conductance fluctuations, δg, against $1/\tau_\phi$ for (a) a 0.8 μm quantum dot and (b) a 0.3 μm dot. The solid dots represent the actual calculations and the lines exponential fits to the data.

In figure 1(a), we plot δg as a function of $1/\tau_\phi$ for a 0.8 μm nominally square quantum dot with the carrier density set to be to a 4×10^{11} cm^{-2}. These parameters were chosen in order to compare with recent experiments done on 1.0 μm split-gate dots. The cavity size was taken as 0.8 μm here in order to account for depletion due to the fringing field induced around the gate edges [3, 5]. The leads were adjusted to permit three propagating modes, again comparable to experiment. The solid dots correspond to the actual calculation and the line corresponds to an exponential fit to the data, which follows the data quite closely. This trend agrees quite nicely with that determined experimentally (as will be discussed below), which also shows exponential decay as a function of $1/\tau_\phi$. In the case of the experiment, values for $1/\tau_\phi$ were determined from the magnetic field dependent evolution of the magneto-resistance fluctuations in the dots, using a simple edge state skipping model [5, 10]. The values of this yields were found to be in good agreement with those of an independent study by Clarke *et al* [3]. The experimental exponential decay constant however is about 30 ps, whereas here the fit yields a value of 28 ± 3 ps. While this agreement is rather good, one must be aware that there are uncertainties in how τ_ϕ is determined experimentally. For theoretical calculations, one *normally* must calculate the conductance by multiplying the zero-temperature results by the derivative of the Fermi

function and integrating with respect to energy, while the calculations presented here only consider the effects of phase breaking on the amplitude of the fluctuations. We will return to this issue of thermal smearing below.

In figure 1(b), δg against $1/\tau_\phi$ is again plotted, but in this case for a 0.3 μm square dot. We have used the same electron density. In this case the number of propagating modes in the leads is two; however this does not change the essential physics. As in the 0.8 μm dot case, the calculations (the dots) appear to follow a decaying exponential (the solid curve), in this case with an overall decay constant of 11 ± 2 ps. That δg should decay more slowly in the smaller dot can probably be attributed in large part to the fact the energy level spacing is larger in the smaller dot, thus a larger V_{in} is required to yield an equivalent effect. It may be noted that the difference in the two values for the decay with phase-breaking time roughly scales as the size of the dot, and not with its area. This is a further indication that the key factor in the fluctuation is the path length along the regular trajectory as it closes upon itself to create the interference that leads to the quantization of the orbit.

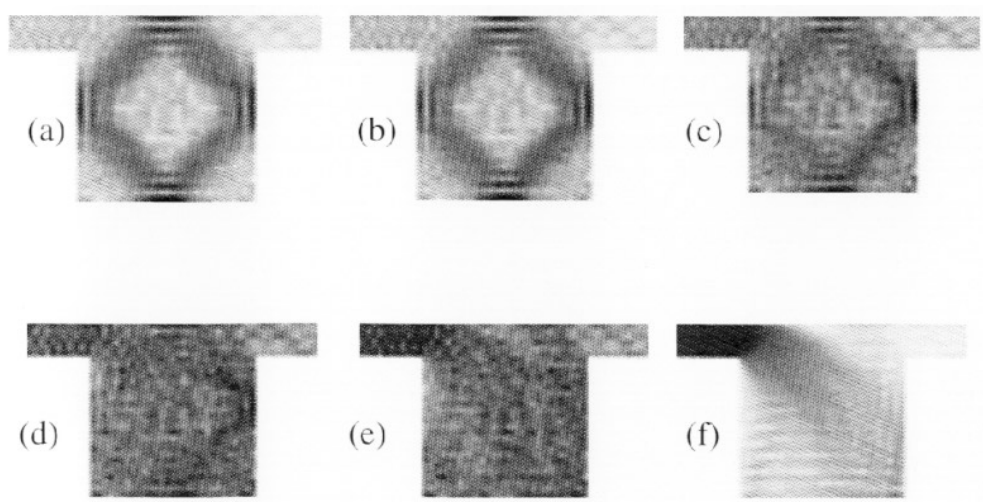

Figure 2. $|\psi(x, y)|$ versus x and y for a 0.3 μm dot at $B = 0.28$ T. Darker shading corresponds to higher amplitude. (a) $\tau_\phi = \infty$; (b) $\tau_\phi = 0.5$ ns; (c) $\tau_\phi = 0.1$ ns; (d) $\tau_\phi = 0.05$ ns; (e) $\tau_\phi = 0.01$ ns; (f) $\tau_\phi = 0.001$ ns.

We now turn to an examination of the wave-functions in these quantum dots in the presence of inelastic scattering. As mentioned earlier, it has been found that the wave-functions show evidence of 'scarring', that is, the amplitudes of the wave-functions are *highly concentrated* along underlying, *single classical trajectories*. The scarring is observed at magnetic fields coincident with resonant maxima or minima in the conductance, but does not necessarily occur at every such feature [8]. This dramatic effect is quite distinct from more usual resonance phenomena, in which the wave-functions typically show a uniform excitation that cannot be associated with single trajectories. An example of this scarring effect is shown in figure 2(a), which shows a plot of $|\psi(x, y)|$ against x and y. The darker shading indicates higher quantum mechanical amplitude. This picture corresponds to the 0.3 μm dot in figure 1, specifically for $B = 0.28$ T and zero temperature. It has been found that this feature appears periodically with period $\Delta B \sim 0.11$ T, which coincides very well with the dominant periodicity that was found generally in the conductance fluctuations, both theoretically and experimentally [6]. The excitation of the modes represented by this figure

corresponds to a swept orbit area in a manner similar to the Aharonov–Bohm criteria, that is $\Delta\phi/\phi_0 = 2\pi$ for the difference in magnetic flux. Then one obtains $A \sim 0.04\ \mu\mathrm{m}^2$ for the enclosed area, which corresponds well with the enclosed area of the diamond scar in figure 2(a).

The subsequent panels in figure 2 show the evolution $|\psi(x, y)|$ for progressively shorter inelastic scattering times. Note the non-linear fashion in which the scarring is disrupted by increasing phase breaking. In particular, reducing τ_ϕ from infinity to 0.5 ns introduces virtually no change in the scarring pattern. In the experiments, 0.5 ns is a typical value for τ_ϕ for temperatures below 100 mK, and in this regime periodic fluctuations due to the striking scarring have been clearly observed [6]. Reducing τ_ϕ by a further factor of five, however, causes a significant disruption of the scarring pattern, although it is still clearly apparent. A further factor of two decrease virtually destroys what remains of the original diamond pattern. As indicated above, the amplitude of the fluctuations typically decays by an order of magnitude on raising the temperature to 1 K, at which point τ_ϕ is typically of the order of 0.05 ns [3, 5]. This corresponds to a inelastic path length $l_\phi = v_F\tau_\phi$ of about 15 μm, still sufficient to make nearly twenty complete circuits of the scarred loop. In other words, the scarring is very sensitively destroyed by phase breaking, as are the associated periodic magneto-resistance fluctuations. Such sensitivity is presumably related to the interference being dominated by the remnant of a single classical orbit. Indeed, in experimental studies of much larger dots, where the characteristics of the interference were consistent with a dense distribution of trajectories contributing to interference, a weaker power law decay was observed by Clarke *et al* [3]. The persistence of the diamond scar up to $\tau_\phi \sim 0.1$ ns also gives an approximate indication of how many circuits or orbits around the scar over which phase coherence must be maintained for this feature to exist, the answer being about forty. Needless to say, the electrons in this case are not taking a direct path between the two leads, and are spending a considerable amount of time in the dot. Despite this, it is evident from the diamond scar that the electrons trajectories are only a *limited portion of the entire area of the dot*. This contrasts strongly with the assumptions made in the semi-classical theory of chaotic dots in which a much more uniform sampling of the dot is assumed [11].

A clue to the dominance of just a single trajectory in the wave-function and why there is an apparent lack of straight-through trajectories comes from inspecting its form for the case of very strong phase breaking. In particular, the emergence of a highly collimated beam from the entrance point contact is apparent for $\tau_\phi = 0.001$ ns. The collimation results from the waveguiding effects of the leads; the entry angle becomes strongly restricted by quantization of the wave-vectors in the y direction when there are just a few propagating modes in the leads. In the final panel, this collimated beam essentially decays before reaching the right-hand boundary of the dot, which is expected since l_ϕ in this instance is less than the distance across the dot.

In figure 3, we compare the decay of the simulated fluctuations with the experimental data as a function of the phase-breaking time. In both cases, the data have been normalized to the values at the lowest data point, so just the decay with phase breaking is apparent. Here, it may be seen that quite good agreement is obtained. This leads to the conclusion that decay of the amplitude of the fluctuations is governed solely by the decay in the phase-breaking time. Another important issue is that the experimental results were obtained for increasingly higher temperatures, while the calculations here are performed for zero temperature. It should be noted however that the experimental method for extracting τ_ϕ involved exploiting its relationship with the correlation field at high magnetic field. The latter was found experimentally to be relatively insensitive to temperature for $T < 1$ K [12].

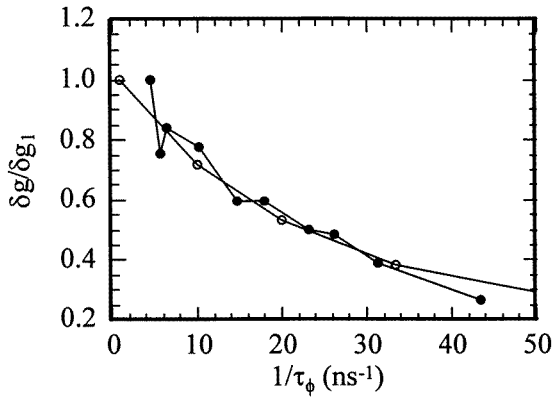

Figure 3. Comparison of the experimental data from a 1.0 μm dot (○), and the theoretical data for the 0.8 μm dot (●). The two data sets are normalized to the first data point at the largest value of the phase-breaking time. The experimental data displayed in figure 3 are combined with results originally published in [4] (see figure 1(b)) and [5] (see figure 4).

Nevertheless, one needs to examine the role of the temperature.

We have also performed finite-temperature calculations for a 0.3 μm dot, which take into account the smearing of the Fermi function derivative. These calculations were performed with slightly wider leads, so that three propagating modes were present. In figure 4, δg against temperature is plotted, with the filled circles corresponding to the absence of inelastic scattering while the open circles and crosses correspond to values of τ_ϕ of 0.1 and 0.05 ns, respectively, with these values held *fixed* across the entire temperature range. The solid lines are the fits obtained assuming an exponential decay law, which our calculations follow quite closely. In fact, the decay constant with respect to temperature in each case is about 0.9 ± 0.1 K^{-1} and the offsetting of the curves where phase breaking is present can be accounted for entirely by multiplying the curve for no inelastic scattering by a factor $\exp(-0.01)/\tau_\phi)$, indicating the exponential behaviour with respect to $1/\tau_\phi$ holds even in the presence of thermal smearing. *Thus, the effects of phase breaking and thermal smearing appear to be separable*.

While the decay of the amplitude of the fluctuations for the 1.0/0.8 μm dot agrees well between theory and experiment in figure 3, there is a difference between the two in terms of the actual amplitude of the fluctuations. The theory can be seen in figure 1(a) to give a value of $\delta g \approx 0.5$, while the experimental value (at the lowest temperature) is about 0.17. To account for this decreased amplitude with an additional thermal smearing would require a temperature of almost 1 K, or an additional phase-breaking process corresponding to a decay of about 40 ns^{-1}. The former is unlikely while the latter is clearly not found in the experiment. In fact, there is no indication from figure 3 that thermal smearing plays any role at all in the temperature dependence of the fluctuations in these regular dots, a result hinted at earlier in discussion of the experimental results. It is expected that, in theoretical discussions of the role of regular semi-classical orbits [13], the dominant decay mechanism of the amplitude of the orbits is that of phase breaking. Because the regular orbits do not represent a sample of the full density of states within the dot, the normal concepts of thermal smearing do not appear to be appropriate to these structures.

One must consider, however, the possibility that the experimental sample is not at the low temperature of the refrigerator. However, it is clear from the measurements

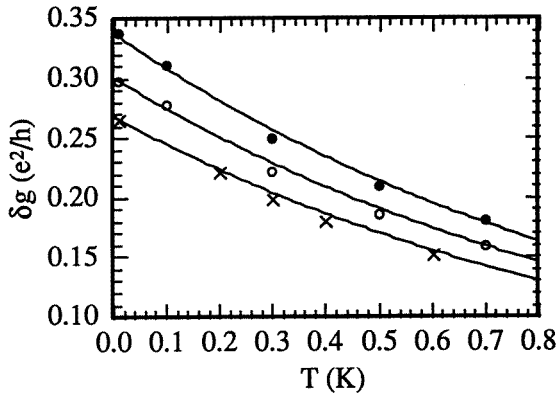

Figure 4. δg against temperature for a 0.3 μm dot for $\tau_\phi = \infty$ (filled circles), $\tau_\phi = 0.1$ ns (open circles) and $\tau_\phi = 0.05$ ns (crosses). The solid lines are exponential fits to the data.

that a temperature variation of the phase-breaking time is being observed at the lowest temperatures, which means that the sample is probably well coupled to the refrigerator heat sink. It is also possible that the device is out of equilibrium. In particular, even with 0.1 nA of current, the resistance of the device would suggest that a voltage drop of several microvolts is appearing across the lead openings. This possible voltage drop is well below that required to induce an energy spread corresponding to the 1 K value inferred above. However, the theory only includes phase breaking *within* the dot. There is also a possibility of phase breaking within the leads, and within the two-dimensional gas outside the dot. These effects would lead to an additional reduction of the amplitude. Further work on the quantitative agreement between experiment and theory is under way.

In conclusion, we have found that the amplitude of the conductance fluctuations in square quantum dots decays exponentially with $1/\tau_\phi$, in good agreement with experiment. The change in the rate of decay with dot size indicates that path length along the regular trajectory is crucial. The scarring of the wave-function, which is tied to the periodicity of the magnetoconductance fluctuations, also reflects the exponential behaviour in $1/\tau_\phi$, as its disruption with respect to τ_ϕ occurs in a highly nonlinear way. In addition, one can look at figure 2 in a somewhat different light, in that as one increases the size of the coherence time, we are in fact observing the *time development* of the transient buildup of the wave-function for carriers injected into the ballistic dot. It is clear that the carriers must be in the dot for a considerable length of time (many orbits) in order for the scar to be developed, and consequently for the periodic oscillations in the magneto-resistance to become fully developed. The decay of the fluctuation amplitude found here, along with the breakup of the scarring, further reinforce the conclusions that these dots are regular structures in which the magnetoconductance is dominated by one, or a few, remnants of semi-classical (regular) orbits that persist within the dot. In regard to this, it should be noted that the diamond shaped scar shown here for the 0.3 μm dot has also been found in the larger 0.8 μm dot. Combining the effects of phase breaking with thermal smearing, we find the latter also causes the fluctuation amplitude to decay exponentially and the two in combination result in a simple addition of decay rates, although we point out that there is no evidence of thermal smearing required to fit the experimental data.

References

[1] For a review see Washburn R and Webb R A 1986 *Adv. Phys.* **35** 375
[2] Marcus C M, Westervelt R M, Hopkins P F and Gossard A C 1993 *Chaos* **3** 643
[3] Clarke R M, Chan I H, Marcus C M, Duruöz C I, Harris J S Jr, Campman K and Gossard A C 1995 *Phys. Rev.* B **52** 2656
[4] Bird J P, Ishibashi K, Aoyagi Y, Sugano T and Ochiai Y 1994 *Phys. Rev.* B **50** 18 678
[5] Bird J P, Ishibashi K, Ferry D K, Ochiai Y and Sugano T 1995 *Phys. Rev.* B **51** 18 037
[6] Bird J P, Ferry D K, Akis R, Ochiai Y, Ishibashi K, Aoyagi Y and Sugano T *Europhys. Lett.* at press
[7] Usuki T, Saito M, Takatsu M, Kiehl R A and Yokoyama N 1995 *Phys. Rev.* B **52** 8244
[8] Akis R, Ferry D K and Bird J P 1996 *Europhys. Lett.* **35** 529
[9] Neofotistos G, Lake R and Datta S 1991 *Phys. Rev.* B **43** 2442
[10] Ferry D K, Edwards G, Yamamoto K, Ochiai Y, Bird J, Ishibashi K, Aoyagi Y and Sugano T 1995 *Japan. J. Appl. Phys.* **34** 4338
[11] Jalabert R A, Baranger H U and Stone A D 1990 *Phys. Rev. Lett.* **65** 2442
[12] Bird J P, Ishibashi K, Ferry D K, Ochiai Y, Aoyagi Y and Sugano T 1995 *Phys. Rev.* B **51** 8295
[13] Ozorio de Almeida A M 1988 *Hamiltonian Systems: Chaos and Quantization* (Cambridge: Cambridge University Press) pp 208–22